

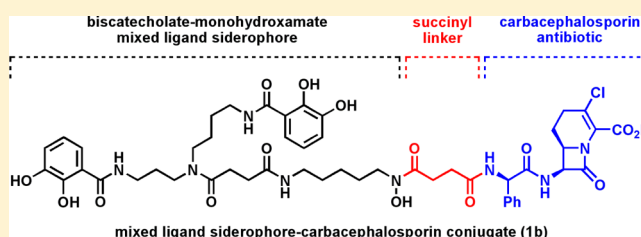
Biscatecholate–Monohydroxamate Mixed Ligand Siderophore–Carbacephalosporin Conjugates are Selective Sideromycin Antibiotics that Target *Acinetobacter baumannii*

Timothy A. Wencewicz and Marvin J. Miller*

Department of Chemistry and Biochemistry, University of Notre Dame, 251 Nieuwland Science Hall, Notre Dame, Indiana 46556, United States

S Supporting Information

ABSTRACT: Chemical syntheses and biological evaluation of biscatecholate–monohydroxamate mixed ligand sideromycins utilizing the carbacephalosporin β -lactam antibiotic loracarbef and the fluoroquinolone antibiotic ciprofloxacin are described. The mixed ligand β -lactam sideromycin (**1b**) had remarkably selective and extremely potent antibacterial activity against the Gram-negative pathogen *Acinetobacter baumannii* ATCC 17961 (MIC = 0.0078 μ M). The antibacterial activity of the β -lactam sideromycin was inversely related to the iron(III) concentration in the testing media and was antagonized by the presence of the competing parent siderophore. These data suggested that active transport of the mixed ligand β -lactam sideromycin across the outer cell membrane of *A. baumannii* via siderophore-uptake pathways was responsible for the selective and potent antibacterial activity.



INTRODUCTION

New antibacterial chemotherapies for treating multidrug-resistant (MDR) Gram-negative bacterial pathogens are desperately needed.¹ The ESKAPE pathogens (*Enterococcus faecium*, *Staphylococcus aureus*, *Klebsiella pneumoniae*, *Acinetobacter baumannii*, *Pseudomonas aeruginosa*, *Enterobacter aerogenes*, *Escherichia coli*) highlighted by the Infectious Disease Society of America (IDSA) attest to the urgency of this public health crisis, as many resistant infections once limited to the hospital setting have spread to the general public.² Among these pathogens, *Acinetobacter baumannii* is being recognized as a rising class of aggressively pathogenic Gram-negative bacteria with the capacity to be MDR.³ New antibiotics to treat MDR *A. baumannii* infections are desperately needed, as there are now clinical strains resistant to every known antibiotic approved for clinical use.⁴

Recent efforts for developing new antibiotic agents against *A. baumannii* have primarily focused on combination therapies with known antibiotic classes.⁵ Other nonconventional therapies applied toward treating MDR Gram-negative infections have also been explored,⁶ including bacterial gene transfer,⁷ bioengineered human tissues that produce defense peptides,⁸ nitric-oxide releasing nanoparticles,⁹ phage therapy,¹⁰ photodynamic therapy,¹¹ radioimmunotherapy,¹² and gallium as an iron-mimetic.¹³ Siderophore-mediated “Trojan Horse” antibiotic drug delivery has been successful at treating highly resistant Gram-negative pathogens because these antibacterial agents overcome membrane permeability barriers¹⁴ by entering cells through active transport mechanisms.¹⁵ The drastic need for new antibiotics against *A. baumannii* inspired us to revisit a mixed ligand biscatecholate–monohydroxamate siderophore–

carbacephalosporin conjugate (**1b**; Figure 1) shown previously by our group¹⁶ to have selective antibacterial activity against *A.*

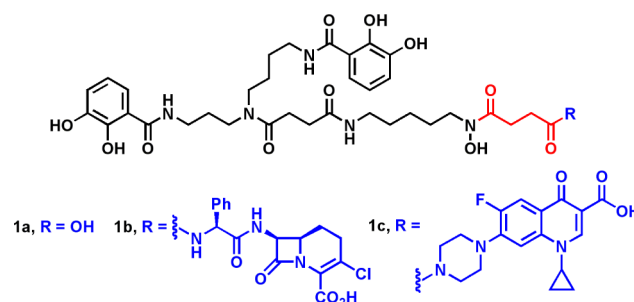


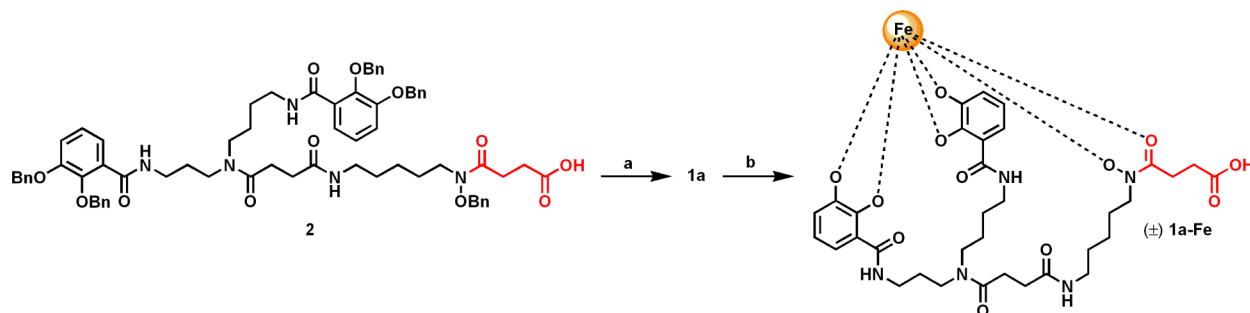
Figure 1. Structures of synthetic mixed ligand siderophore (**1a**) and synthetic sideromycins (**1b** and **1c**) used in this work.

baumannii. In this work, we provide insight on the mechanism of action of conjugate **1b** and show that the impressive antibacterial potency against *A. baumannii* (MIC = 0.0078 μ M) results from its active transport through siderophore transport proteins.

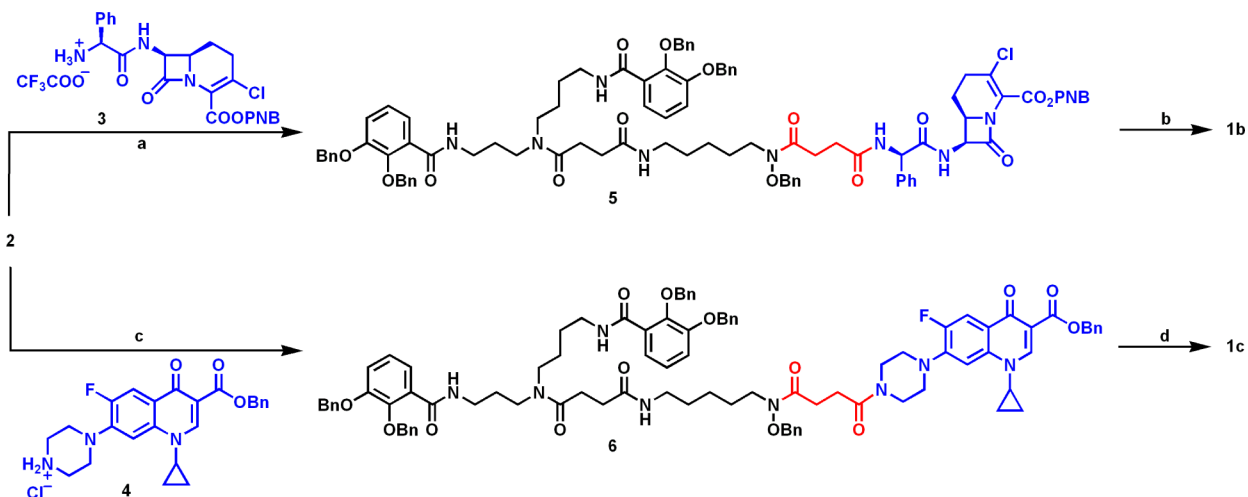
To date, the most successful siderophore–antibiotic conjugates (synthetic sideromycins¹⁷) against Gram-negative bacteria have featured β -lactam antibiotics as the warhead.¹⁸ The β -lactam antibiotics have been particularly useful in this area because their penicillin binding protein (PBP) biological targets are in the periplasm.¹⁹ This means that the siderophore

Received: February 20, 2013

Published: April 24, 2013

Scheme 1. Syntheses of Iron-Free (1a) and Iron-Bound (1a-Fe) Mixed Ligand Siderophores^a

^aReagents and conditions: (a) 10% Pd–C, H₂ (1 atm), MeOH, 26 h, 90%; (b) Fe(acac)₃, MeOH, 2 h, 98%.

Scheme 2. Syntheses of Mixed Ligand Sideromycins 1b and 1c^a

^aReagents and conditions: (a) EDC, 3, *i*Pr₂EtN, DMAP, CH₂Cl₂, 24 h, 52%; (b) 10% Pd–C, H₂ (1 atm), HCl (3 equiv), DMF:H₂O (95:5), 24 h, 68%; (c) EDC, 4, *i*Pr₂EtN, DMAP, CH₂Cl₂, 24 h, 52%; (d) 10% Pd–C, H₂ (1 atm), MeOH, 24 h, 51%.

only needs to smuggle the antibiotic across the outer membrane and not all the way into the cytoplasm. For this study, we designed a siderophore–fluoroquinolone conjugate (**1c**; Figure 1) with a cytoplasmic antibiotic target (DNA gyrase¹⁹) for direct comparison with the siderophore– β -lactam conjugate (**1b**).

RESULTS AND DISCUSSION

Syntheses of Siderophores and Sideromycins. The synthesis of penta-*O*-benzyl-protected siderophore **2** was accomplished using a literature protocol previously described by our group.²⁰ The iron-free (**1a**) and iron-complexed (**1a-Fe**) siderophores were synthesized as shown in Scheme 1. Palladium-catalyzed hydrogenolysis of protected siderophore **2** in MeOH gave the universally deprotected mixed ligand siderophore **1a** in excellent yield and purity after recrystallization from MeOH/Et₂O. Treatment of siderophore **1a** with Fe(acac)₃ in MeOH gave a quantitative yield of the siderophore–Fe(III) complex as a purple solid after recrystallization from MeOH/Et₂O.

The syntheses of the benzyl protected siderophore–antibiotic conjugates **5** and **6** were accomplished by coupling suitably protected antibiotics **3** and **4** to the free carboxyl terminus of protected siderophore **2** (Scheme 2). The protected antibiotics were prepared according to previously reported literature protocols.^{16,21} Derivatization of the free

amines of the carbacephalosporin β -lactam antibiotic, loracarbef, and the fluoroquinolone antibiotic, ciprofloxacin, with large molecules, including siderophores, is well tolerated, and the resulting conjugates still retain affinity for the protein target in vitro.²² Carbodiimide-mediated amide formation between *O*-PNB-loracarbef TFA salt **3** and protected siderophore **2** under basic conditions provided the fully protected β -lactam conjugate **5**. Similar reaction between *O*-benzyl-ciprofloxacin (**4**) and the protected siderophore **2** gave fully *O*-benzyl protected ciprofloxacin conjugate **6**.

Universal deprotection of the *O*-PNB and *O*-benzyl protecting groups from conjugate **5** was achieved using optimized hydrogenolysis conditions described for this system previously (Scheme 2).¹⁶ The deprotection proceeded in high yield as anticipated, but the tedious purification of β -lactam sideromycin **1b** reported previously¹⁶ needed to be improved to provide higher compound purity for biological studies. A new purification protocol was developed using sequential purifications by size exclusion chromatography, preparative HPLC, and recrystallization from MeOH/Et₂O to provide analytically pure material (see the Experimental Section and Supporting Information for complete experimental details, characterization data, and purity analysis). Universal deprotection of the *O*-benzyl protecting groups from conjugate **6** was achieved using conventional Pd-catalyzed hydrogenolysis conditions (Scheme 2). The fluoroquinolone sideromycin **1c**

Table 1. MIC Values (μM) of Compounds 1a, 1a-Fe, 1b, and 1c against ESKAPE Panel of Bacteria^{a,b}

entry	compd	<i>E. faecium</i> NCTC 7171	<i>S. aureus</i> SG 511	<i>K. pneumoniae</i> ATCC 700603	<i>A. baumannii</i> ATCC 17961	<i>P. aeruginosa</i> ATCC 27853	<i>E. aerogenes</i> ATCC 35029	<i>E. coli</i> ATCC 25922
1	1a	>128	>128	>128	>128	>128	>128	>128
2	1a-Fe	>128	>128	>128	>128	>128	>128	>128
3	1b	>128	32	>128	0.125	>128	>128	8
4	1c	>128	>128	>128	>128	>128	>128	>128
5	loracarbef	32	1	128	>128	>128	>128	2
6	ciprofloxacin	8	0.5	0.25	0.25	0.125	<0.015	<0.015

^aMIC values were determined using the broth microdilution method using visual end point analysis according to the CLSI guidelines.²³ ^bEach compound was tested in triplicate.

was recrystallized from MeOH/Et₂O, which provided analytically pure material with no need for chromatographic purification.

Antibacterial Activity of Siderophores and Sideromycins against ESKAPE Pathogens. The mixed ligand β -lactam sideromycin 1b was reported previously by our group to have unexpected selective potency toward *Acinetobacter baumannii*.¹⁶ To confirm this activity, the mixed ligand siderophore 1a, siderophore–Fe(III) complex 1a-Fe, sideromycin 1b, sideromycin 1c, and control antibiotics loracarbef and ciprofloxacin were evaluated in a broth microdilution antibacterial susceptibility assay against an ESKAPE panel of pathogenic Gram-positive and Gram-negative bacteria (Table 1). The siderophores (1a and 1a-Fe) had no growth inhibiting activity (MIC values >128 μM) against all of the organisms, which was expected because the siderophores should be growth promoting factors for the bacteria. The β -lactam sideromycin 1b gave moderate MIC values against *S. aureus* (32 μM) and *E. coli* (8 μM) and a selectively potent MIC value of 0.125 μM against *A. baumannii*, which was in agreement with the previously reported antibacterial data.¹⁶ The parent β -lactam antibiotic, loracarbef, displayed a much different spectrum of antibiotic activity and had no activity against *A. baumannii* (MIC value >128 μM). The fluoroquinolone sideromycin 1c had no antibacterial activity against all the bacterial strains tested, while the parent fluoroquinolone antibiotic, ciprofloxacin, showed the expected broad spectrum activity.

Effect of Competing Siderophores and Fe(III) Concentration on Sideromycin Antibacterial Activity. The drastic difference in the spectrum of antibacterial activity for the β -lactam sideromycin 1b and the parent antibiotic loracarbef was the first indication that sideromycin 1b was being transported via siderophore-uptake pathways. If sideromycin 1b was truly entering bacterial cells via siderophore-associated pathways, then the antibacterial activity should be antagonized by the parent siderophore (1a) and its corresponding Fe(III) complex (1a-Fe).²⁴ This antagonistic effect was indeed observed in a siderophore–sideromycin antagonism assay performed on agar media. As shown in Figure 2a, the antibacterial activity of sideromycin 1b against *A. baumannii* ATCC 17961 was antagonized at the intersection points with siderophore 1a and its Fe(III) complex 1a-Fe. This observation was consistent with active transport of sideromycin 1b by *A. baumannii* into the periplasm where the β -lactam could interact with its PBP biological target and cause cell death. Interestingly, Figure 2b shows that siderophores 1a and 1a-Fe had no antagonistic effects on the antibiotic activity of sideromycin 1b against *S. aureus* SG511, a Gram-positive strain of bacteria. This phenomenon was consistent with an extracellular β -lactam

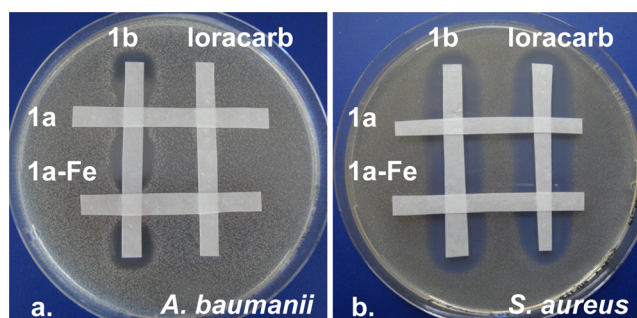


Figure 2. Agar diffusion antagonism assay for sideromycin 1b and siderophores 1a and 1a-Fe tested against (a) *A. baumannii* ATCC 17961 and (b) *S. aureus* SG511. Images are not shown to actual scale.

target in *S. aureus*, where active transport into *S. aureus* cells is not required for reaching the PBP biological target.¹⁹

Antagonism of the anti-*A. baumannii* activity of sideromycin 1b by competing siderophores²⁴ and Fe(III) supplementation^{18d,25} was also observed using a Kirby–Bauer²⁶ agar diffusion assay²⁷ (Figure 3). As shown in Figure 3a,

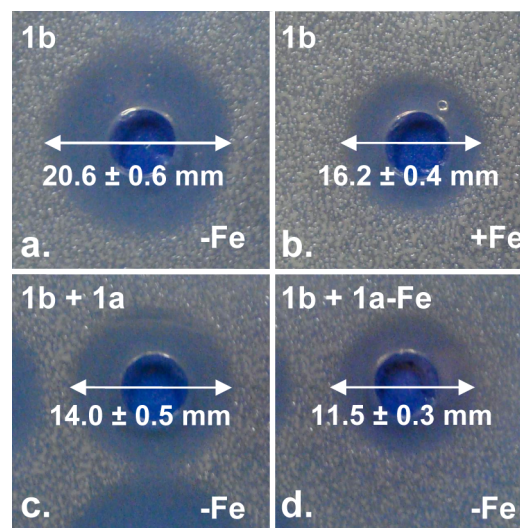


Figure 3. Agar diffusion antibacterial susceptibility assay for sideromycin 1b against *A. baumannii* ATCC 17961. Growth inhibition zones for 1b under Fe(III)-deficient conditions (MHII agar + 100 μM BIPY) (a), for 1b under Fe(III)-supplemented conditions (MHII agar + 100 μM FeCl₃) (b), for a 1:1 molar mixture of 1b and 1a under Fe(III)-deficient conditions (c), and for a 1:1 mixture of 1b and 1a-Fe under Fe(III)-deficient conditions (d). Images are shown at relative but not actual scale. Measured zone diameters are the average of three independent trials. See the Supporting Information (Table S2) for tabulated data.

sideromycin **1b** produced a growth inhibition zone with a diameter of 20.6 mm in media made deficient in Fe(III) by addition of 100 μM 2,2'-bipyridine (BIPY). As shown in Figure 3b, addition of 100 μM FeCl_3 to the testing media reduced the diameter of the growth inhibition zone to 16.2 mm. The inverse relationship between Fe(III) availability and antibacterial potency of sideromycin **1b** against *A. baumannii* was consistent with siderophore-related active transport across the outer membrane.²⁵ Additionally, the antagonistic effects of siderophore **1a** and its Fe(III) complex **1a-Fe** were confirmed in the agar diffusion assay. As shown in parts c and d of Figure 3, 1:1 molar ratios of sideromycin **1b** and siderophore **1a** or Fe(III) complex **1a-Fe**, respectively, gave statistically reduced diameters of growth inhibition in Fe(III)-deficient media relative to **1b** alone (Figure 3a).

The results from Figure 3 are summarized graphically in Figure 4 by plotting the diameter of the growth inhibition zone

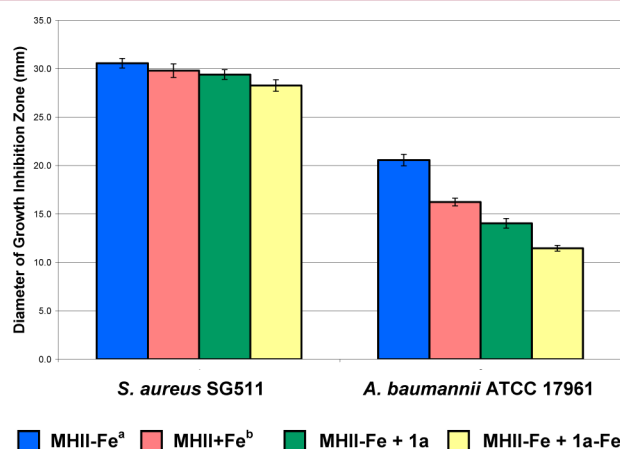


Figure 4. Effect of varying Fe(III) concentrations and competing siderophores (**1a** and **1a-Fe**) on the antibacterial activity of sideromycin **1b** against *S. aureus* SG511 and *A. baumannii* ATCC 17961 in the agar diffusion assay. The vertical axis indicates the diameter of the growth inhibition zone in millimeters (average of three independent trials), and the horizontal axis indicates the test organism. See the Supporting Information (Table S2) for tabulated data. ^aMHII-Fe: Mueller–Hinton agar no. 2 + 100 μM BIPY. ^bMHII+Fe: Mueller–Hinton agar no. 2 + 100 μM FeCl_3 .

on the vertical axis under the assay conditions specified by the color coded legend. Analogous experiments were performed using **1b** against a Gram-positive pathogen, *S. aureus* SG511. The activity against *S. aureus* was not significantly perturbed by varying the Fe(III) concentration in the testing media or under competition conditions with an equimolar amount of parent siderophore (**1a**) or Fe(III) complex (**1a-Fe**). These results are consistent with the lack of antagonism observed in Figure 2 and again suggest that active transport is not necessary to reach the *S. aureus* extracellular PBP target of the β -lactam warhead.¹⁹ In contrast, the testing results against *A. baumannii* (discussed previously when referring to Figure 3) show a clear dependence on Fe(III) concentration and antagonism by **1a** and **1a-Fe** consistent with active transport of **1b**.

The influence of Fe(III) concentration and competing siderophores on the antibacterial activity of sideromycin **1b** was further quantified by determining MIC values using a broth microdilution assay (Table 2). In Fe(III)-supplemented Mueller–Hinton no. 2 broth media (MHII+Fe), sideromycin **1b** produced an MIC value of 0.5 μM against *A. baumannii*,

Table 2. MIC Values (μM) of Sideromycin (**1b**) against *A. baumannii* and *S. aureus* under Varying Concentrations of Fe(III) and in the Presence of Competing Siderophores (**1a** and **1a-Fe**)^{a,b}

entry	compd	test organism			
		<i>A. baumannii</i> ATCC 17961		<i>S. aureus</i> SG511	
		MHII+Fe ^c	MHII-Fe ^d	MHII+Fe	MHII-Fe
1	1b	0.5	0.0078	64	32
2	1b + 1a	nt ^e	0.0312	nt	16
3	1b + 1a-Fe	nt	0.25	nt	32

^aMIC values were determined using the broth microdilution method using visual end point analysis according to the CLSI guidelines.²³

^bEach compound was tested in triplicate. ^cMHII+Fe: Mueller–Hinton broth no. 2 + 100 μM FeCl_3 . ^dMHII-Fe: Mueller–Hinton broth no. 2 + 100 μM BIPY. ^ent: not tested.

while in Fe(III)-deficient media (MHII-Fe), the MIC was 0.0078 μM . This represents a 64-fold increase in activity when going from Fe(III)-supplemented to Fe(III)-deficient conditions. When 1:1 molar mixtures of sideromycin:siderophore, **1b:1a** and **1b:1a-Fe**, were tested, MIC values of 0.031 and 0.25 μM , respectively, were recorded. These results were in agreement with data from the agar diffusion assays (Figures 3 and 4) where the siderophore Fe(III)-complex **1a-Fe** antagonized the antibacterial activity of sideromycin **1b** to a greater extent than the iron-free siderophore **1a**. As expected, the antibacterial activity of sideromycin **1b** against *S. aureus* was not influenced to any great extent by the addition Fe(III) or siderophores (**1a** and **1a-Fe**) to the media.

FURTHER DISCUSSION AND PERSPECTIVE

To better understand the highly potent and selective activity of sideromycin **1b** against *A. baumannii*, it was important to consider what is known about the organism's natural use of siderophores. The complete genome sequences of six *A. baumannii* strains have recently been reported, and genome analysis revealed that siderophore biosynthetic genes were present in 5 out of the 6 sequenced strains.²⁸ The strain lacking the siderophore biosynthetic genes was the only nonclinical isolate of *A. baumannii* sequenced, which suggested that siderophores are an important virulence factor for *A. baumannii* during infection. So far, three biosynthetic gene clusters for unique siderophores have been identified in *A. baumannii*,²⁹ and the structures of two classes of these siderophores, (pre)acinetobactin³⁰ and fimsbactins³¹ (Figure 5), have been elucidated.

Interestingly, both (pre)acinetobactin and the fimsbactins are mixed ligand siderophores containing catecholate and hydroxamate iron(III)-chelating ligands (Figure 5). Much is known about acinetobactin assembly^{30d,e} and trafficking,^{30b,c} but it is still unclear whether preacinetobactin or acinetobactin is the biologically active siderophore. The structural similarity of (pre)acinetobactin to the siderophores anguibactin, pseudomonine, vibriobactin, pyochelin, and yersiniabactin suggests that it might also form a 1:1 siderophore:iron complex with oxygen and nitrogen atoms from the catecholate, hydroxamate, oxazoline, and imidazole ring participating in iron(III) chelation.³² With this unique structural type of metal complex, it is unlikely that the synthetic mixed-ligand siderophore **1a** and sideromycin **1b** (which presumably utilize two catecholates and one hydroxamate to make a 1:1 complex with iron) from this

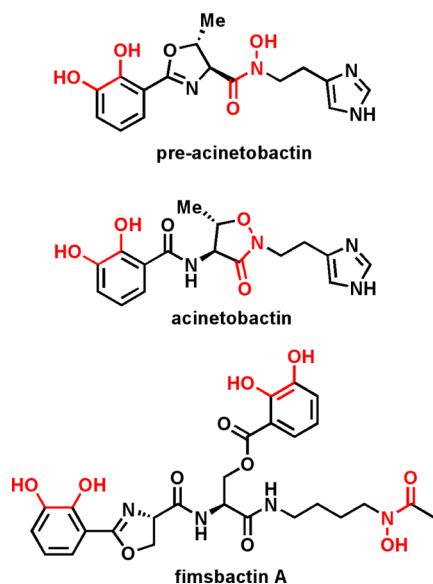


Figure 5. Structures of mixed ligand siderophores (preacinetobactin, acinetobactin, and fimsbactin A) produced by *A. baumannii*. Catechol and hydroxamic acid iron(III)-chelating groups are shown in red.

work share the same membrane transport system as (pre)-acinetobactin in *A. baumannii*, but at this point it cannot be ruled out.

A recent publication reported the structures, biosynthetic genes, and membrane transport genes of the fimsbactins, a new class of siderophores from *A. baumannii*.³¹ The structure of the fimsbactins are remarkably similar to the synthetic mixed ligand siderophore **1a** used in this study. Both structures contain two catechols and one hydroxamic acid ligand arranged in a similar order and architecture. While no structural information is currently available, it is possible that the synthetic siderophore **1a** and sideromycin **1b** mixed ligand iron(III) complexes mimic the fimsbactin–iron(III) complexes. As a result, these siderophore–iron(III) complexes might share the same uptake pathway in *A. baumannii*, which could explain the high sensitivity of *A. baumannii* to the mixed ligand biscatecholate–monohydroxamate– β -lactam sideromycin **1b**. Additionally, the transcription of all the siderophore biosynthetic and transport genes in *A. baumannii* are under the genetic control of a ferric uptake regulator (Fur) protein, which helps rationalize the inverse correlation of anti-*A. baumannii* activity and Fe(III) concentration observed for sideromycin **1b** in this study.^{29b} Further investigation to see if the synthetic mixed ligand biscatecholate–monohydroxamate siderophore **1a** and sideromycin **1b** utilize fimsbactin or acinetobactin transport systems in *A. baumannii* would be of great value for optimizing the therapeutic approach of siderophore-mediated antibiotic delivery described in this work.

The mixed ligand–fluoroquinolone sideromycin **1c** showed no antibacterial activity against all the strains tested (Table 1). As discussed previously, the mixed ligand– β -lactam sideromycin **1b** was transported by Gram-negative bacteria, such as *A. baumannii*, across the outer membrane into the periplasm where its PBP biological target is located. The lack of antibacterial activity of the mixed ligand–fluoroquinolone sideromycin **1c** suggested that it was never transported across the inner membrane of *A. baumannii* into the cytoplasm where the fluoroquinolone's biological target, DNA gyrase, is located. On the basis of the well established structure–activity

relationships of the fluoroquinolone antibiotics, it is unlikely that covalent modification of the ciprofloxacin warhead in conjugate **1c** diminished all ability to inhibit DNA gyrase. It is well-known that the C-7 position of the fluoroquinolone scaffold is the most forgiving in terms of bulky modifications.³³ In the case of ciprofloxacin, the presence of a secondary or tertiary amine is optimal, but the distal nitrogen of the piperazine unit can be alkylated or acylated and still inhibit DNA gyrase with great potency; even when derivatized with large/siderophores such as pyoverdine from *Pseudomonas aeruginosa* as proven by Abdallah and co-workers.^{22b} On the basis of these arguments, it is more likely that mixed ligand synthetic sideromycin **1c** was not trafficked to the cytoplasm in *A. baumannii*. This suggests that sideromycins built around mixed ligand siderophore **1a** that target Gram-negative bacteria should feature antibiotics with periplasmic targets (Figure 6).

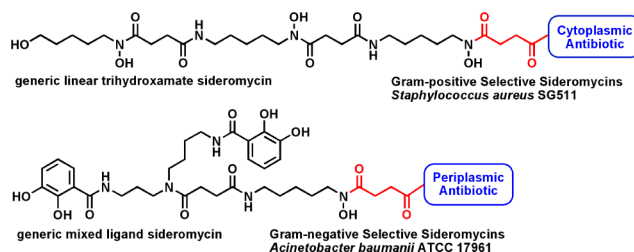


Figure 6. A generic trihydroxamate sideromycin selective for Gram-positive pathogens^{35a,b} and a generic mixed ligand sideromycin selective for Gram-negative pathogens (this work).

We previously reported siderophore–fluoroquinolone conjugates based on trihydroxamate siderophores from the ferrioxamine family with selectively potent activity against Gram-positive bacteria, including *S. aureus*, able to transport ferrioxamine siderophores to the cytoplasm.³⁴ Therefore, antibiotics with cytoplasmic targets might be reserved for sideromycins that target Gram-positive bacteria (Figure 6). The problem of delivering antibacterial drugs to the cytoplasm of Gram-negative bacteria with siderophore delivery vectors remains to be solved. One general method to expand the scope of antibacterial agents available for use in siderophore-mediated drug delivery is to design new microbe-triggered linker systems that selectively release the antibiotic warhead near the desired site of action.³⁵

SUMMARY AND CONCLUSIONS

New antibacterial treatments for MDR *A. baumannii* are desperately needed as strains resistant to every known antibiotic are beginning to spread.^{3,4} The mixed ligand siderophore– β -lactam conjugate **1b** described here represents an important new agent that kills *A. baumannii* with exceptional nanomolar potency (MIC = 0.0078 μ M) and selectivity in whole cell antibacterial assays. To evaluate the usefulness in continuing the development of sideromycin **1b** as a potential chemotherapeutic treatment for *A. baumannii* infections, the antibacterial activity against clinical MDR isolates of *A. baumannii* and efficacy in mouse infection models are currently being pursued.

EXPERIMENTAL SECTION

Materials and Instrumentation. Reactions were conducted under an atmosphere of dry argon unless otherwise stated. All solvents and reagents were obtained from commercial sources and

used without further purification unless otherwise stated. Dichloromethane (CH_2Cl_2) was distilled from calcium hydride. Dimethylformamide (DMF) and diisopropylethylamine ($i\text{Pr}_2\text{EtN}$) were used from Acros Seal anhydrous bottles. Pentabenzyl-biscatechol–monohydroxamate siderophore **2** was prepared according to a previously described method.²⁰ Protected antibiotics **3** and **4** were prepared as described previously.^{16,21,34} Sorbent Technologies silica gel 60 (32–63 μm) was used for all silica gel column chromatography purifications.

All microbiological media and liquids were sterilized before use by autoclaving at 121 °C for at least 15 min unless otherwise stated. Distilled, deionized, and filtered water (Millipore Milli-Q Advantage A10 water purification system) was used to prepare all aqueous solutions and media. Luria broth (LB) was purchased from VWR. Mueller–Hinton no. 2 broth (MHII broth; cation adjusted) was purchased from Sigma-Aldrich (St. Louis, MO). Mueller–Hinton no. 2 agar (MHII agar; HiMedia Laboratories) was purchased from VWR. McFarland BaSO_4 turbidity standards were purchased from bioMérieux, Inc. Sterile plastic Petri dishes (145 mm \times 20 mm; Greiner Bio-One) and sterile polystyrene 96-well plates (BD Falcon) used for antibacterial susceptibility testing were purchased from VWR. Ferric chloride (anhydrous, reagent grade), and 2,2'-bipyridine (reagent plus grade) were purchased from Sigma-Aldrich.

^1H NMR and ^{13}C NMR spectra were recorded on a 600 MHz Varian DirectDrive spectrometer, and FID data was processed using ACD/ChemSketch version 10.04. Chemical shifts (δ) are reported in parts per million (ppm) and are referenced to residual solvent. Coupling constants (J) are reported in hertz (Hz).

High resolution, accurate mass measurements were obtained with a Bruker micrOTOF II electrospray ionization time-of-flight mass spectrometer in positive ion mode using direct sample injection. Sample was introduced via flow injection at a rate of 4 $\mu\text{L}/\text{min}$, and mass spectra were accumulated from 50 to 3000 m/z for 2 min.

HPLC-MS was performed on a Waters ZQ instrument consisting of a chromatography module Alliance HT, photodiode array detector 2996, and mass spectrometer Micromass ZQ with an MS electrospray source operated at a capillary voltage of 3.5 kV and a desolvation temperature of 300 °C. A YMC Pro C18 reverse phase column (3.0 mm \times 50 mm) fit with a 0.5 μm precolumn frit and a YMC Pro C18 guard column (2.0 mm \times 10 mm) was used for all analyses. Mobile phases used were 0.1% TFA in H_2O (A) and 0.1% TFA in CH_3CN (B). A gradient was formed from 5%–80% of B in 10 min, then 80%–95% of B in 2 min, and then 95%–5% of B in 3 min at a flow rate of 0.7 mL/min (total run time of 15 min).

Preparative HPLC purifications were performed on a Waters preparative binary pump system at a flow rate of 15 mL/min with UV detection at 280 nm using a YMC-Pack Pro C18 column (150 mm \times 20 mm; 5 μm particle size) fit with a guard column. Mobile phases used were 0.1% TFA in H_2O (A) and 0.1% TFA in CH_3CN (B). A gradient was formed from 30%–60% of B over 4 min, then 60%–90% of B over 0.25 min, and was held at 90% of B for 0.75 min.

Thin layer chromatography (TLC) was performed with Al-backed Merck 60-F₂₅₄ or Al-backed Merck RP-C18 F₂₅₆ silica gel plates using a 254 nm lamp and aqueous FeCl_3 for visualization. Melting points were determined in capillary tubes using a Thomas–Hoover melting point apparatus and are uncorrected. The purity of compounds tested in biological assays was evaluated by analytical HPLC and verified to be $\geq 95\%$, unless otherwise noted.

Preparation of Fe(III)-Supplemented and Fe(III)-Depleted Media. Iron-deficient and iron-supplemented media prep has been described previously by our group³⁴ and is summarized again here. Iron-deficient MHII broth (MHII–Fe) was prepared by adding 0.8 mL of a 1 mg/mL filter-sterilized aqueous solution of 2,2'-bipyridine to 49.2 mL of sterile MHII broth. Iron-supplemented MHII broth (MHII+Fe) was prepared by adding 0.8 mL of a freshly prepared 1 mg/mL filter-sterilized aqueous solution of FeCl_3 to 49.2 mL of sterile MHII broth. Iron-deficient MHII agar (MHII–Fe) was prepared by adding 0.5 mL of a 1 mg/mL filter-sterilized aqueous solution of 2,2'-bipyridine to 34 mL of melted MHII agar with gentle mixing. Iron-supplemented MHII agar (MHII+Fe) was prepared by adding 0.5 mL

of a freshly prepared 1 mg/mL filter-sterilized aqueous solution of FeCl_3 to 34 mL of melted MHII agar with gentle mixing.

MIC Determination by the Broth Microdilution Assay. Minimum inhibitory concentrations (MICs) were determined using the broth microdilution method according to the Clinical and Laboratory Standards Institute (CLSI, formerly the NCCLS) guidelines²³ and as described previously by our group.^{27,34} The specific details of this assay are provided in the Supporting Information.

Paper Strip Agar Diffusion Siderophore–Sideromycin Competition Assay. A general version of this assay has been described previously by our group,³⁴ and the specific procedure used in this work is provided. Cultures of *S. aureus* SG511 and *A. baumannii* ATCC 17961 were grown in LB broth for 18–24 h, and standard cell suspensions of 1.5×10^6 CFU/mL were prepared in saline solution (0.9% NaCl) according to a 0.5 BaSO_4 McFarland Standard.³⁶ Each standardized suspension (0.1 mL) was added to 34 mL of sterile, melted MHII–Fe agar tempered to 47 °C. After gentle mixing, the inoculated agar media was poured into a sterile plastic Petri dish (145 mm \times 20 mm) and allowed to solidify near a flame with the lid cracked for ~ 30 min. Solutions of the test compounds dissolved in a 1:10 mixture of DMSO:MeOH (**1a**, **1a-Fe**, and **1b**) or sterile, distilled, and deionized H_2O (loracarbef) were prepared at the desired concentration (2.0 mM for **1a** and **1a-Fe**, 0.5 mM for **1b**, 1.0 mM and 0.1 mM for loracarbef against *A. baumannii* and *S. aureus*, respectively). Sterile filter paper strips (Whatman no. 1 standard grade, cut to ~ 1 cm \times 8 cm) were soaked in the test compound and laid on the surface of the inoculated agar media as shown in Figure 2. The Petri dishes were incubated at 37 °C for 18–24 h and then stored at rt until being photographed at the 48 h time point.

Modified Kirby–Bauer Agar Diffusion Antibiotic Susceptibility Assay. A modified Kirby–Bauer agar diffusion assay was used to assess compound antibacterial activity.³⁶ Details of this assay have been reported previously by our group and can be found in the Supporting Information.^{27,34}

Procedures for the Syntheses of Siderophores and Sideromycins. *Biscatechol–Monohydroxamate Siderophore (1a).* Compound **2** (145.0 mg, 0.12 mmol) was dissolved in 15 mL of MeOH in an HCl-washed 25 mL round-bottom flask sealed under argon. The flask was charged with 10% Pd–C (30.0 mg) and exposed to a balloon of hydrogen gas (~ 1 atm). Reaction progress was monitored by RP-C18 TLC (1.5:1 $\text{CH}_3\text{CN}:\text{H}_2\text{O}$; FeCl_3 stain), and after 26 h there was no remaining starting material (**2**). The flask was flushed with argon, and the mixture was vacuum filtered through Celite. Evaporation of the MeOH gave a white solid that was recrystallized from MeOH/Et₂O to provide the desired siderophore (**1a**) in 90% yield (80.5 mg, 0.11 mmol); mp 71–73 °C (color change), 150–160 °C (dec). ^1H NMR (600 MHz, CD_3OD) δ 7.23–7.19 (m, 2 H), 6.94–6.90 (m, 2 H), 6.73–6.68 (m, 2 H), 3.61–3.54 (m, 2 H), 3.48–3.40 (m, 4 H), 3.38 (t, $J = 6.2$ Hz, 2 H), 3.35 (t, $J = 6.5$ Hz, 2 H), 3.12 (t, $J = 6.7$ Hz, 2 H), 2.74 (t, $J = 6.6$ Hz, 2 H), 2.67 (dt, $J = 17.2, 6.6$ Hz, 2 H), 2.58–2.53 (m, 2 H), 2.52–2.44 (m, 2 H), 1.96 (dt, $J = 14.6, 7.2$ Hz, 1 H), 1.82 (ddd, $J = 13.2, 6.5, 6.2$ Hz, 1 H), 1.75–1.54 (m, 6 H), 1.51–1.43 (m, 2 H), 1.34–1.25 (m, 2 H). HRMS-ESI (m/z): $[\text{M} + \text{H}]^+$ calcd for $\text{C}_{34}\text{H}_{48}\text{N}_5\text{O}_{12}$, 718.3294; found, 718.3278. Note: The ^{13}C NMR spectrum in CD_3OD and DMSO- d_6 shows rotamers resulting in a complex mixture of ^{13}C -signals.

Biscatechol–Monohydroxamate Siderophore–Iron(III) Complex (1a-Fe). Siderophore **1a** (10.0 mg, 0.015 mmol) and $\text{Fe}(\text{acac})_3$ (5.9 mg, 0.017 mmol) were dissolved in 5 mL of MeOH. The purple solution was heated at 40 °C (oil bath temperature) for 2 h. The MeOH was removed under reduced pressure, and the purple residue was dissolved in a minimal amount of MeOH and then precipitated by addition of Et₂O. The desired siderophore–iron(III) complex (**1a-Fe**) was isolated in 98% yield as a purple solid (11.5 mg, 0.015 mmol); mp >260 °C. HRMS-ESI (m/z): $[\text{M} + 3\text{H}]^+$ calcd for $\text{C}_{33}\text{H}_{45}\text{FeN}_5\text{O}_{12}$, 771.2409; found, 771.2416. HPLC-MS retention time of 1.65 min. Note: The iron(III)-complex **1a-Fe** was insoluble in pure water, many common organic solvents (EtOAc, CH_2Cl_2 , CHCl_3 , Et₂O, CH_3CN , MeOH), and mixed water/organic solvent systems ($\text{H}_2\text{O}/\text{MeOH}$, $\text{H}_2\text{O}/\text{CH}_3\text{CN}$). The iron(III)-complex **1a-Fe** was highly soluble in

DMSO, DMF, and weakly basic aqueous solutions (5% NaHCO₃ in H₂O).

Penta-O-benzyl-biscatechol-Monohydroxamate-O-PNB-Loracarbef Conjugate (5). The synthesis of this compound has been reported previously by a slightly different synthetic approach.¹⁶ O-PNB-loracarbef TFA salt (3; 208.0 mg, 0.35 mmol) was dissolved in 5 mL of anhydrous CH₂Cl₂, and the solution was cooled to 0 °C (ice bath temp). An excess of iPr₂EtN (0.40 mL, 2.3 mmol) was slowly added under argon, followed directly by a catalytic amount of DMAP (7.0 mg, 0.06 mmol), a solution of benzyl-protected siderophore 2 (450.0 mg, 0.38 mmol) in 10 mL of CH₂Cl₂, and EDC-HCl (136.0 mg, 0.71 mmol), respectively. The mixture was warmed to rt and stirred overnight under dry argon. After 24 h, TLC (3% MeOH in CH₂Cl₂; FeCl₃ stain) showed no remaining starting material (3). The CH₂Cl₂ was evaporated under reduced pressure, and the resulting oil was partitioned between 50 mL of EtOAc and 50 mL of 1 N HCl. The layers were separated, and the EtOAc was washed with 25 mL of H₂O. All the aqueous layers were combined and extracted with 50 mL of EtOAc. The EtOAc layers were combined and washed with 50 mL of brine, dried over MgSO₄, gravity filtered, and concentrated under reduced pressure. This gave 650 mg of a viscous oil that was purified via silica gel column chromatography (1.25 in. × 4 in. silica gel; 3–5% MeOH in EtOAc). Pure benzyl-protected mixed ligand siderophore-loracarbef conjugate (5) was obtained in 52% yield as an off-white, waxy solid (302.5 mg, 0.18 mmol); mp 70–72 °C. ¹H NMR (600 MHz, DMSO-*d*₆) δ 9.32 (br s, 1 H), 9.11 (d, *J* = 8.5 Hz, 1 H), 8.88 (br s, 1 H), 8.82 (br s, 1 H), 8.63 (d, *J* = 7.6 Hz, 1 H), 8.27–8.21 (m, 2 H), 7.77 (br s, 1 H), 7.69 (d, *J* = 8.8 Hz, 1 H), 7.51–7.03 (m, 35 H), 6.75 (d, *J* = 10.3 Hz, 1 H), 6.66 (s, 1 H), 5.48 (d, *J* = 7.6 Hz, 1 H), 5.46–5.35 (m, 5 H), 5.20–5.08 (m, 2 H), 5.07–4.98 (m, 2 H), 4.92–4.82 (m, 2 H), 3.95–3.73 (m, 4 H), 3.59–3.47 (m, 2 H), 3.33–3.07 (m, 8 H), 2.99–2.91 (m, 2 H), 2.62 (ddd, *J* = 18.8, 12.1, 6.3 Hz, 4 H), 2.55–2.44 (m, 4 H), 2.34–2.23 (m, 2 H), 1.85–0.98 (m, 12 H). HRMS-ESI (*m/z*): [M + Na]⁺ calcd for C₉₂H₉₆ClN₉NaO₁₇, 1656.6505; found, 1656.6538. Note: The ¹³C NMR spectrum in DMSO-*d*₆ shows rotamers resulting in a complex mixture of ¹³C signals.

Biscatechol-Monohydroxamate-Loracarbef Conjugate (1b).

The synthesis of this compound has been reported previously by a slightly different synthetic approach.¹⁶ Benzyl-protected conjugate 5 (209.5 mg, 0.13 mmol) was dissolved in 2.50 mL of DMF:H₂O (95/5; v/v) in an HCl-washed round-bottom flask. Concentrated HCl (33.4 μL, 0.38 mmol) and 10% Pd-C (41.9 mg) were added, respectively, and the flask was sealed under argon. The flask was then flushed several times with hydrogen gas using intermediate vacuum evacuations, and the mixture was left stirring at rt under a balloon of hydrogen gas (~1 atm). Reaction progress was monitored by RP-C18 TLC (1.5:1 CH₃CN:H₂O; FeCl₃ stain), and after 24 h there was no remaining starting material (5) and a new product appeared giving a strong FeCl₃ positive test was present (*R*_f 0.78; purple with FeCl₃ stain). The flask was flushed with argon, and the mixture was vacuum filtered through glass filter paper. The DMF and H₂O were removed using high vacuum rotary evaporation (~1 mmHg), which gave 250 mg of a viscous oil. This material was purified by size exclusion chromatography (Sephadex LH20, 10.0 g; 10% MeOH in EtOAc). Several fractions of varying purity (70–90% pure by analytical HPLC) were isolated from the size exclusion column, and each fraction (Fr) was recrystallized from MeOH/Et₂O to give the desired conjugate in 68% yield as off-white solids: Fr 1 (17.5 mg), Fr 2 (44.8 mg), Fr 3 (19.5 mg), Fr 4 (10.0 mg). A portion of the largest fraction (Fr 2; 30 mg) was subjected to purification by preparative HPLC (see Materials and Instrumentation for exact details of purification) where the desired compound 1b elutes at 4.15 min. Pure fractions were lyophilized, and the obtained solid was recrystallized from MeOH/Et₂O to give 15 mg of an analytically pure sample of conjugate 1b as a white-solid used for spectral characterization and biological testing; mp 123–125 °C (color change), 186–188 °C (dec). ¹H NMR (600 MHz, CD₃OD) δ 7.44–7.28 (m, 5 H), 7.23–7.18 (m, 2 H), 6.94–6.90 (m, 2 H), 6.73–6.68 (m, 2 H), 5.41 (d, *J* = 8.8 Hz, 1 H), 5.36 (d, *J* = 4.7 Hz, 1 H), 3.89–3.84 (m, 1 H), 3.81 (ddd, *J* = 13.9, 7.2, 7.0 Hz, 1 H), 3.47–3.32 (m, 8

H), 3.25 (td, *J* = 13.4, 6.6 Hz, 1 H), 3.16–3.09 (m, 2 H), 2.85–2.81 (m, 2 H), 2.71–2.47 (m, 8 H), 2.43–2.36 (m, 1 H), 1.98–1.92 (m, 1 H), 1.79 (ddd, *J* = 13.6, 6.7, 6.6 Hz, 1 H), 1.76–1.68 (m, 2 H), 1.68–1.52 (m, 6 H), 1.52–1.42 (m, 2 H), 1.32–1.23 (m, 2 H). ¹³C NMR (150 MHz, CD₃OD) δ 175.6, 175.6, 174.9, 174.9, 174.6, 174.6, 174.1, 173.9, 171.8, 171.7, 171.6, 171.6, 166.4, 163.6, 150.6, 150.5, 150.4, 150.4, 147.5, 147.5, 147.5, 147.5, 138.3, 138.2, 130.8, 130.7, 130.6, 130.2, 130.0, 129.7, 129.5, 129.4, 129.4, 129.0, 125.6, 124.7, 119.8, 119.8, 119.7, 119.7, 118.8, 118.7, 118.7, 118.6, 116.9, 116.9, 116.8, 116.8, 74.0, 59.9, 59.7, 59.6, 54.1, 46.9, 46.9, 44.6, 40.5, 40.2, 40.0, 38.1, 37.7, 32.5, 32.2, 32.2, 31.3, 29.8, 29.8, 29.7, 29.5, 29.5, 28.9, 28.6, 27.9, 27.8, 27.2, 27.1, 26.2, 24.8, 24.7, 23.1. HRMS-ESI (*m/z*): [M + H]⁺ calcd for C₅₀H₆₂ClN₈O₁₅, 1049.4018; found, 1049.4010. HPLC-MS retention time of 5.75 min.

Penta-O-benzyl-biscatechol-Monohydroxamate-O-Benzyl-ciprofloxacin Conjugate (6). O-Benzyl-ciprofloxacin hydrochloride salt (4) was free-based using Amberlite IR400(OH⁻) resin in CHCl₃ for 4 h. The resulting O-benzyl-ciprofloxacin amine (45.0 mg, 0.11 mmol), penta-O-benzyl-biscatechol-monohydroxamate 2 (117.0 mg, 0.10 mmol), iPr₂EtN (0.04 mL, 0.23 mmol), DMAP (3.0 mg, 0.025 mmol), and EDC-HCl (31.0 mg, 0.16 mmol) were dissolved in 5 mL of anhydrous CH₂Cl₂, respectively. After 24 h at rt, TLC (6% MeOH in CH₂Cl₂; FeCl₃ stain) showed no remaining starting material 2. The mixture was diluted with CH₂Cl₂ (35 mL), washed with H₂O (30 mL), saturated aqueous NaHCO₃ (30 mL), and brine (30 mL), dried over anhydrous MgSO₄, filtered, and concentrated. The crude product was purified by silica gel column chromatography (1 in. × 5 in. silica gel; 3–5% MeOH in CHCl₃) to give the desired product (6) in 52% yield as a clear wax (80.9 mg, 0.05 mmol). ¹H NMR (600 MHz, CDCl₃) δ 8.53–8.46 (m, 1 H), 8.36–8.18 (m, 1 H), 8.09–7.85 (m, 3 H), 7.73–7.57 (m, 1 H), 7.54–7.00 (m, 32 H), 6.97–6.51 (m, 4 H), 6.41 (d, *J* = 4.1 Hz, 1 H), 6.31 (br s, 1 H), 5.40–5.36 (m, 2 H), 5.17–4.96 (m, 8 H), 4.91–4.86 (m, 2 H), 3.86–3.75 (m, 2 H), 3.75–3.55 (m, 4 H), 3.51–3.35 (m, 3 H), 3.34–3.03 (m, 10 H), 2.87–2.75 (m, 2 H), 2.71–2.39 (m, 6 H), 2.16–1.90 (m, 2 H), 1.75–1.31 (m, 12 H), 1.13–1.00 (m, 2 H). ¹³C NMR (150 MHz, CDCl₃) δ 173.7, 173.2, 173.0, 172.3, 172.2, 172.0, 171.7, 171.6, 171.3, 170.4, 169.7, 165.4, 165.3, 165.2, 165.1, 165.1, 165.0, 154.1, 152.4, 151.6, 151.6, 151.6, 148.3, 147.8, 146.8, 146.7, 146.5, 144.0, 137.9, 136.5, 136.3, 136.3, 136.3, 136.2, 129.1, 129.0, 128.8, 128.8, 128.8, 128.7, 128.7, 128.6, 128.6, 128.6, 128.6, 128.5, 128.5, 128.4, 128.4, 128.4, 128.2, 128.2, 128.2, 128.1, 127.9, 127.9, 127.8, 127.8, 127.8, 127.6, 127.6, 127.5, 127.3, 127.3, 127.3, 127.3, 127.0, 126.0, 124.4, 124.4, 124.3, 124.2, 123.3, 123.1, 123.1, 123.0, 122.8, 117.9, 117.7, 116.8, 116.5, 115.1, 113.4, 113.2, 110.0, 105.1, 76.4, 76.4, 76.3, 76.2, 76.1, 71.2, 71.0, 71.0, 71.0, 66.3, 50.0, 49.5, 47.2, 45.1, 41.4, 39.2, 38.9, 38.7, 38.5, 37.0, 36.9, 34.5, 31.5, 28.6, 27.2, 26.6, 26.6, 26.3, 25.9, 24.9, 23.8, 22.6, 8.1. HRMS-ESI (*m/z*): [M + Na]⁺ calcd for C₉₃H₉₉FN₈NaO₁₄, 1593.7157; found, 1593.7155.

Biscatechol-Monohydroxamate-Ciprofloxacin Conjugate (1c).

Penta-O-benzyl-biscatechol-monohydroxamate-O-benzyl-ciprofloxacin conjugate (6; 75.0 mg, 0.05 mmol) was dissolved in 8 mL of MeOH:EtOAc (3:1) in an HCl-washed, 10 mL round-bottom flask sealed under argon. The flask was charged with 10% Pd-C (18.5 mg) and exposed to a balloon of hydrogen gas (~1 atm). Reaction progress was monitored by RP-C18 TLC (1.5:1 CH₃CN:H₂O; FeCl₃ stain), and after 24 h there was no remaining starting material (6) and a new product appeared giving a strong FeCl₃ positive test was present (*R*_f 0.44; purple with FeCl₃ stain). The flask was flushed with argon, and the mixture was diluted with MeOH, vacuum filtered through Celite, and concentrated under reduced pressure to give a tan film. The film was dissolved in MeOH and the product (1c) precipitated as a faint purple solid after addition of cold Et₂O. The desired conjugate (1c) was obtained in 51% yield as a faint purple solid (25.0 mg, 0.025 mmol); mp 131–134 °C (dec). ¹H NMR (600 MHz, CD₃OD) δ 8.74 (s, 1 H), 7.95 (d, *J* = 13.8 Hz, 1 H), 7.54 (br s, 1 H), 7.22–7.17 (m, 2 H), 6.89–6.85 (m, 2 H), 6.68–6.61 (m, 2 H), 3.83–3.77 (m, 4 H), 3.71 (br s, 1 H), 3.63–3.56 (m, 2 H), 3.48–3.32 (m, 12 H), 3.13 (t, *J* = 6.9 Hz, 2 H), 2.82 (t, *J* = 5.7 Hz, 2 H), 2.74–2.63 (m, 4 H), 2.48 (dt, *J* = 13.7, 6.8 Hz, 2 H), 1.98–1.91 (m, 2 H), 1.81 (dt, *J* = 14.1, 7.0 Hz,

2 H), 1.75–1.69 (m, 2 H), 1.69–1.54 (m, 4 H), 1.53–1.44 (m, 2 H), 1.40–1.34 (m, 2 H), 1.34–1.27 (m, 2 H). HRMS-ESI (m/z): $[M + H]^+$ calcd for $C_{51}H_{64}FN_8O_{14}$, 1031.4521; found, 1031.4522. HPLC-MS retention time of 7.76 min. Note: The ^{13}C NMR spectrum in CD_3OD and $DMSO-d_6$ shows rotamers resulting in a complex mixture of ^{13}C -signals.

■ ASSOCIATED CONTENT

■ Supporting Information

Complete list of strains, markers, and origins for microorganisms used in this work. Complete list of antibiotic susceptibility testing data from the agar diffusion assay. Copies of 1H NMR and ^{13}C NMR spectra for compounds **1a**, **1b**, **1c**, **2**, **5**, and **6**. Copies of HPLC-MS chromatograms for compounds subjected to biological testing (**1a-Fe**, **1b**, and **1c**). This material is available free of charge via the Internet at <http://pubs.acs.org>.

■ AUTHOR INFORMATION

Corresponding Author

*Phone: 574-631-7571. Fax: 574-631-6652. E-mail: mmiller1@nd.edu

Notes

The authors declare no competing financial interest.

■ ACKNOWLEDGMENTS

We gratefully acknowledge the use of NMR facilities provided by the Lizzadro Magnetic Resonance Research Center at The University of Notre Dame (UND) and the mass spectrometry services provided by The UND Mass Spectrometry & Proteomics Facility (N. Sevova, Dr. W. Boggess, and Dr. M. V. Joyce; supported by the National Science Foundation under CHE-0741793). We thank Prof. Shariar Mobashery (UND) and Dr. Sergei Vakulenko (UND) for providing the *ESKAPE* panel of bacteria and Dr. Nuno Tiago Gao Antunes for some initial antibiotic susceptibility testing. Partial funding for this work was provided by NIH grant AI054193. T.A.W. gratefully acknowledges The UND Chemistry–Biochemistry–Biology (CBB) Interface Program funded by NIH (T32GM075762) for three years of fellowship support. T.A.W. thanks UND Department of Chemistry and Biochemistry (Grace Fellowship), the Center for Environmental Science and Technology (CEST), and Bayer for additional support.

■ ABBREVIATIONS USED

acac, acetylacetonate; ATCC, American Type Culture Collection; BIPY, 2,2'-bipyridine; Bn, benzyl; Boc, *tert*-butoxycarbonyl; DMAP, 4-dimethylaminopyridine; DMF, dimethylformamide; DMSO, dimethylsulfoxide; EDC, 1-ethyl-3-(3-dimethylaminopropyl)carbodiimide; Fur, ferric uptake regulator; HPLC, high-performance liquid chromatography; HRMS, high-resolution mass spectrometry; MDR, multidrug-resistant; MHII, Mueller–Hinton media no. II; MIC, minimum inhibitory concentration; NMR, nuclear magnetic resonance; PBP, penicillin binding protein; PNB, *para*-nitrobenzyl; TFA, trifluoroacetic acid

■ REFERENCES

- (1) Fischback, M. A.; Walsh, C. T. Antibiotics for emerging pathogens. *Science* **2009**, *325*, 1089–1093.
- (2) Boucher, H. W.; Talbot, G. H.; Bradley, J. S.; Edwards, J. E., Jr.; Gilbert, D.; Rice, L. B.; Scheld, M.; Spellberg, B.; Bartlett, J. Bad bugs,

no drugs: No *ESKAPE*! An update from the Infectious Diseases Society of America. *Clin. Infect. Dis.* **2009**, *48*, 1–12.

- (3) (a) Visca, P.; Seifert, H.; Towner, K. J. *Acinetobacter* infection—an emerging threat to human health. *IUBMB Life* **2011**, *63*, 1048–1054. (b) Peleg, A. Y.; Seifert, H.; Paterson, D. L. *Acinetobacter baumannii*: emergence of a successful pathogen. *Clin. Microbiol. Rev.* **2008**, *21*, 538–582.

- (4) Vila, J.; Pachón, J. *Acinetobacter baumannii* resistant to everything: What should we do? *Clin. Microbiol. Infect.* **2011**, *17*, 955–956.

- (5) (a) Bassetti, M.; Repetto, E.; Righi, E.; Boni, S.; Diverio, M.; Molinari, M. P.; Mussap, M.; Artioli, S.; Ansaldi, F.; Durando, P.; Orenco, G.; Bobbio Pallavicini, F.; Viscoli, C. Colistin and rifampicin in the treatment of multidrug-resistant *Acinetobacter baumannii* infections. *J. Antimicrob. Chemother.* **2008**, *61*, 417–420. (b) Lee, N. Y.; Wang, C. L.; Chuang, Y. C.; Yu, W. L.; Lee, H. C.; Chang, C. M.; Wang, L. R.; Ko, W. C. Combination carbapenem–sulbactam therapy for critically ill patients with multidrug-resistant *Acinetobacter baumannii* bacteremia: four case reports and an in vitro combination synergy study. *Pharmacotherapy* **2007**, *27*, 1506–1511.

- (6) Radu Mihai, M.; Martinez, L. R. Novel therapies for treatment of multidrug-resistant *Acinetobacter baumannii* skin infections. *Virulence* **2011**, *2*, 97–102.

- (7) Shankar, R.; He, L. K.; Szilagy, A.; Muthu, K.; Gamelli, R. L.; Filutowicz, M.; Wendt, J. L.; Suzuki, H.; Dominguez, M. A novel antibacterial gene transfer treatment for multidrug-resistant *Acinetobacter baumannii*-induced burn sepsis. *J. Burn Care Res.* **2007**, *28*, 6–12.

- (8) Thomas-Virnig, C. L.; Centanni, J. M.; Johnston, C. E.; He, L. K.; Schlosser, S. J.; Van Winkle, K. F.; Chen, R.; Gibson, A. L.; Szilagy, A.; Li, L.; Shankar, R.; Allen-Hoffmann, B. L. Inhibition of multidrug-resistant *Acinetobacter baumannii* by nonviral expression of hCAP-18 in a bioengineered human skin tissue. *Mol. Ther.* **2009**, *17*, S62–S69.

- (9) Friedman, A. J.; Han, G.; Navati, M. S.; Chacko, M.; Gunther, L.; Alfieri, A.; Friedman, J. M. Sustained release nitric oxide releasing nanoparticles: characterization of a novel delivery platform based on nitrite containing hydrogel/glass composites. *Nitric Oxide* **2008**, *19*, 12–20.

- (10) Lin, N. T.; Chiou, P. Y.; Chang, K. C.; Chen, L. K.; Lai, M. J. Isolation and characterization of phi AB2: a novel bacteriophage of *Acinetobacter baumannii*. *Res. Microbiol.* **2010**, *161*, 308–314.

- (11) Dai, T.; Tegos, G. P.; Lu, Z.; Huang, L.; Zhiyentayev, T.; Franklin, M. J.; Baer, D. G.; Hamblin, M. R. Photodynamic therapy for *Acinetobacter baumannii* burn infections in mice. *Antimicrob. Agents Chemother.* **2009**, *53*, 3929–3934.

- (12) Dadachova, E.; Casadevall, A. Antibodies as delivery vehicles for radioimmunotherapy of infectious diseases. *Expert Opin. Drug Delivery* **2005**, *2*, 1075–1084.

- (13) Antunes, L. C.; Imperi, F.; Minandri, F.; Visca, P. In vitro and in vivo antimicrobial activity of gallium nitrate against multidrug resistant *Acinetobacter baumannii*. *Antimicrob. Agents Chemother.* **2012**, *56*, S961–S970.

- (14) Vila, J.; Martí, S.; Sánchez-Céspedes, J. Porins, efflux pumps and multidrug resistance in *Acinetobacter baumannii*. *J. Antimicrob. Chemother.* **2007**, *59*, 1210–1215.

- (15) (a) Ji, C.; Juárez-Hernández, R. E.; Miller, M. J. Exploiting bacterial iron acquisition: siderophore conjugates. *Future Med. Chem.* **2012**, *4*, 297–313. (b) Möllmann, U.; Heinisch, L.; Bauernfeind, A.; Köhler, T.; Ankel-Fuchs, D. Siderophores as drug delivery agents: application of the “Trojan Horse” strategy. *Biometals* **2009**, *22*, 615–624.

- (16) Ghosh, A.; Ghosh, M.; Niu, C.; Malouin, F.; Moellmann, U.; Miller, M. J. Iron transport-mediated drug delivery using mixed-ligand siderophore– β -lactam conjugates. *Chem. Biol.* **1996**, *3*, 1011–1019.

- (17) Braun, V.; Pramanik, A.; Gwinner, T.; Köberle, M.; Bohn, E. Sideromycins: tools and antibiotics. *Biometals* **2009**, *22*, 3–13.

- (18) (a) Ji, C.; Miller, P. A.; Miller, M. J. Iron transport-mediated drug delivery: practical syntheses and in vitro antibacterial studies of tris-catecholate siderophore–aminopenicillin conjugates reveals selectively potent antipseudomonal activity. *J. Am. Chem. Soc.* **2012**, *134*,

- 9898–9901. (b) Flanagan, M. E.; Brickner, S. J.; Manjinder, L.; Casavant, J.; Deschenes, L.; Finegan, S. M.; George, D. M.; Granskog, K.; Hardink, J. R.; Huband, M. D.; Hoang, T.; Lamb, L.; Marra, A.; Mitton-Fry, M.; Mueller, J. P.; Mullins, L. M.; Noe, M. C.; O'Donnell, J. P.; Pattavina, D.; Penzien, J. B.; Schuff, B. P.; Sun, J.; Whipple, D. A.; Young, J.; Gootz, T. D. Preparation, Gram-negative antibacterial activity, and hydrolytic stability of novel siderophore-conjugated monocarbam diols. *ACS Med. Chem. Lett.* **2011**, *2*, 385–390. (c) Page, M. G. P.; Dantier, C.; Desarbre, E. In vitro properties of BAL30072, a novel siderophore sulfactam with activity against multiresistant Gram-negative bacilli. *Antimicrob. Agents Chemother.* **2010**, *54*, 2291–2302. (d) Heinisch, L.; Wittmann, S.; Stoiber, T.; Berg, A.; Ankel-Fuchs, D.; Möllmann, U. Highly antibacterial active aminoacyl penicillin conjugates with bis-catecholate siderophores based on secondary diamino acids and related compounds. *J. Med. Chem.* **2002**, *45*, 3032–3040.
- (19) Walsh, C. *Antibiotics: Actions, Origins, and Resistance*; ASM Press: Washington, DC, 2003.
- (20) Ghosh, M.; Miller, M. J. Synthesis and in vitro antibacterial activity of spermidine-based mixed catechol- and hydroxamate-containing siderophore–vancomycin conjugates. *Bioorg. Med. Chem.* **1996**, *4*, 43–48.
- (21) Jung, M. E.; Yang, E. C.; Vu, B. T.; Kiankarimi, M.; Spyrou, E.; Kaunitz, J. Glycosylation of fluoroquinolones through direct oxygenated polymethylene linkages as a sugar-mediated active transport system for antimicrobials. *J. Med. Chem.* **1999**, *42*, 3899–3909.
- (22) (a) Brochu, A.; Brochu, N.; Nicas, T. I.; Parr, T. R., Jr.; Minnick, A. A., Jr.; Dolence, E. K.; McKee, J. A.; Miller, M. J.; Lavoie, M. C.; Malouin, F. Modes of action and inhibitory activities of new siderophore– β -lactam conjugates that use specific iron uptake pathways for entry into bacteria. *Antimicrob. Agents Chemother.* **1992**, *36*, 2166–2175. (b) Hennard, C.; Truong, Q. C.; Desnottes, J.-F.; Paris, J.-M.; Moreau, N. J.; Abdallah, M. A. Synthesis and activities of pyoverdine–quinolone adducts: a prospective approach to a specific therapy against *Pseudomonas aeruginosa*. *J. Med. Chem.* **2001**, *44*, 2139–2151.
- (23) *Methods for Dilution: Antimicrobial Susceptibility Tests for Bacteria That Grow Aerobically*, 8th ed.; CLSI: Villanova, PA, 2009.
- (24) Pramanik, A.; Braun, V. Albomycin uptake via a ferric hydroxamate transport system of *Streptococcus pneumoniae* R6. *J. Bacteriol.* **2006**, *188*, 3878–3886.
- (25) de Lorenzo, V.; Perez-Martín, J.; Escobar, L.; Pesole, G.; Bertoni, G., Mode of binding of the Fur protein to target DNA: negative regulation of iron-controlled gene expression. In *Iron Transport in Bacteria*; Crosa, J. H., Mey, A. R., Payne, S. M., Eds.; ASM Press: Washington, D.C., 2004; pp 185–196.
- (26) Bauer, A. W.; Kirby, W. M. M.; Sherris, J. C.; Turck, M. Antibiotic susceptibility testing by a standardized single disk method. *Am. J. Clin. Pathol.* **1966**, *45*, 493–496.
- (27) Wenciewicz, T. A.; Yang, B.; Rudloff, J. R.; Oliver, A. G.; Miller, M. J. N–O Chemistry for antibiotics: discovery of N-alkyl-N-(pyridin-2-yl)hydroxylamine scaffolds as selective antibacterial agents using nitroso Diels–Alder and ene chemistry. *J. Med. Chem.* **2011**, *54*, 6843–6858.
- (28) (a) Adams, M. D.; Goglin, K.; Molyneaux, N.; Hujer, K. M.; Lavender, H.; Jamison, J. J.; MacDonald, I. J.; Martin, K. M.; Russo, T.; Campagnari, A. A.; Hujer, A. M.; Bonomo, R. A.; Gill, S. R. Comparative genome sequence analysis of multidrug-resistant *Acinetobacter baumannii*. *J. Bacteriol.* **2008**, *190*, 8053–8064. (b) Iacono, M.; Villa, L.; Fortini, D.; Bordoni, R.; Imperi, F.; Bonnal, R. J.; Sicheritz-Ponten, T.; De Bellis, G.; Visca, P.; Cassone, A.; Carattoli, A. Whole-genome pyrosequencing of an epidemic multidrug-resistant *Acinetobacter baumannii* strain belonging to the European clone II group. *Antimicrob. Agents Chemother.* **2008**, *52*, 2616–2625. (c) Smith, M. G.; Gianoulis, T. A.; Pukatzki, S.; Mekalanos, J. J.; Ornston, L. N.; Gerstein, M.; Snyder, M. New insights into *Acinetobacter baumannii* pathogenesis revealed by high-density pyrosequencing and transposon mutagenesis. *Genes Dev.* **2007**, *21*, 601–614. (d) Vallenet, D.; Nordmann, P.; Barbe, V.; Poirel, L.; Mangenot, S.; Bataille, E.; Dossat, C.; Gas, S.; Kreimeyer, A.; Lenoble, P.; Oztas, S.; Poulain, J.; Segurens, B.; Robert, C.; Abergel, C.; Claverie, J. M.; Raoult, D.; Médique, C.; Weissenbach, J.; Cruveiller, S. Comparative analysis of *Acinetobacter*: three genomes for three lifestyles. *PLoS One* **2008**, *3*, e1805.
- (29) (a) Antunes, L. C. S.; Imperi, F.; Towner, K. J.; Visca, P. Genome-assisted identification of putative iron-utilization genes in *Acinetobacter baumannii* and their distribution among a genotypically diverse collection of clinical isolates. *Res. Microbiol.* **2011**, *162*, 279–284. (b) Eijkelkamp, B. A.; Hassan, K. A.; Paulsen, I. T.; Brown, M. H. Investigation of the human pathogen *Acinetobacter baumannii* under iron limiting conditions. *BMC Genomics* **2011**, *12*, 126–139.
- (30) (a) Yamamoto, S.; Okujo, N.; Sakakibara, Y. Isolation and structure elucidation of acinetobactin, a novel siderophore from *Acinetobacter baumannii*. *Arch. Microbiol.* **1994**, *162*, 249–254. (b) Dorsey, C. W.; Tomaras, A. P.; Connerly, P. L.; Tolmasky, M. E.; Crosa, J. H.; Actis, L. A. The siderophore-mediated iron acquisition systems of *Acinetobacter baumannii* ATCC 19606 and *Vibrio anguillarum* 775 are structurally and functionally related. *Microbiology* **2004**, *150*, 3657–3667. (c) Mihara, K.; Tanabe, T.; Yamakawa, Y.; Funahashi, T.; Nakao, H.; Narimatsu, S.; Yamamoto, S. Identification and transcriptional organization of a gene cluster involved in biosynthesis and transport of acinetobactin, a siderophore produced by *Acinetobacter baumannii* ATCC 19606. *Microbiology* **2004**, *150*, 2587–2597. (d) Sattely, E. S.; Walsh, C. T. A Latent Oxazoline Electrophile for N–O–C Bond Formation in Pseudomonine Biosynthesis. *J. Am. Chem. Soc.* **2008**, *130*, 12282–12284. (e) Wuest, W. M.; Sattely, E. S.; Walsh, C. T. Three Siderophores from One Bacterial Enzymatic Assembly Line. *J. Am. Chem. Soc.* **2009**, *131*, 5056–5057. (f) Takeuchi, Y.; Ozaki, S.; Satoh, M.; Mimura, K.-I.; Hara, S.-I.; Abe, H.; Nishioka, H.; Harayama, T. Synthesis of Acinetobactin. *Chem. Pharm. Bull.* **2010**, *58*, 1552–1553.
- (31) Proschak, A.; Lubuta, P.; Grün, P.; Löhr, F.; Wilharm, G.; De Berardinis, V.; Bode, H. B. Structure and Biosynthesis of Fimsbactins A–F, Siderophores from *Acinetobacter baumannii* and *Acinetobacter baylyi*. *ChemBioChem* **2013**, *14*, 633–638.
- (32) Crosa, J. H.; Walsh, C. T. Genetics and Assembly Line Enzymology of Siderophore Biosynthesis in Bacteria. *Microbiol. Mol. Biol. Rev.* **2002**, *66*, 223–249.
- (33) Mitscher, L. A. Bacterial Topoisomerase Inhibitors: Quinolone and Pyridone Antibacterial Agents. *Chem. Rev.* **2005**, *105*, 559–592.
- (34) Wenciewicz, T. A.; Long, T. E.; Möllmann, U.; Miller, M. J. Trihydroxamate Siderophore–Fluoroquinolone Conjugates are Selective Sideromycin Antibiotics that Target *Staphylococcus aureus*. *Bioconjugate Chem.* **2013**, *24*, 473–486.
- (35) (a) Ji, C.; Miller, M. J. Chemical syntheses and in vitro antibacterial activity of two desferrioxamine B–ciprofloxacin conjugates with potential esterase and phosphatase triggered drug release linkers. *Bioorg. Med. Chem.* **2012**, *20*, 3828–3836. (b) Wenciewicz, T. A.; Möllmann, U.; Long, T. E.; Miller, M. J. Is drug release necessary for antimicrobial activity of siderophore–drug conjugates? Syntheses and biological studies of the naturally occurring salmicycin “Trojan Horse” antibiotics and synthetic desferrioxamine–antibiotic conjugates. *Biomaterials* **2009**, *22*, 633–648. (c) Zheng, T.; Bullock, J. L.; Nolan, E. M. Siderophore-Mediated Cargo Delivery to the Cytoplasm of *Escherichia coli* and *Pseudomonas aeruginosa*: Syntheses of Monofunctionalized Enterobactin Scaffolds and Evaluation of Enterobactin–Cargo Conjugate Uptake. *J. Am. Chem. Soc.* **2012**, *134*, 18388–18400.
- (36) Murray, P. R.; Baron, E. J.; Pfaller, M. A.; Tenover, F. C.; Tenover, R. H. *Manual of Clinical Microbiology*. 7th ed.; American Society for Microbiology: Washington, DC, 1999.